Vol 4, Issue 3, March 2024 www.ijesti.com E-ISSN: 2582-9734
International Journal of Engineering, Science, Technology and Innovation (IJESTI)

" Fluid-Structure Interaction Analysis of Francis Turbines Under Sediment Erosion Conditions"

Satyam Kumar Mohapatra [1]

Research Scholar, Department of M. Tech Thermal Engineering,
Sri Satya Sai University of Technology and Medical Sciences, Bhopal, M.P, India.

Dr Sachin Baraskar [2]

Research Guide, Department of M. Tech Thermal Engineering,
Sri Satya Sai University of Technology and Medical Sciences, Bhopal, M.P, India.

ABSTRACT

Sediment erosion is one of the key challenges in hydraulic turbines from a design and maintenance perspective in Himalayas. The present study focuses on choosing the best design in terms of blade angle distribution of a Francis turbine runner which has least erosion effect without influencing the efficiency and the structural integrity. A fully coupled Fluid-Structure-Interaction (FSI) analysis was performed through a multi-field solver, which showed that the maximum stress induced in the optimized design for better sediment handling, is less than that induced in the reference design. Some numerical validation techniques have been shown for both CFD and FSI analysis.

1. Introduction

Nepal's tropical climate, immature geology, and intense seasonal rainfall contribute significantly to sediment-induced degradation of hydraulic turbine components, particularly through erosion and sedimentation. Southeast Asia alone accounts for two-thirds of the global sediment transport to oceans, exacerbating the erosion challenges faced by hydroelectric infrastructure in the region. The erosive potential of sediments is largely determined by their quartz content, which possesses sufficient hardness to damage turbine materials. Despite the presence of sediment settling and flushing systems in hydropower plants, Francis turbines continue to suffer from severe erosion. In particular, the inlet region of the runner is vulnerable due to high pressure differentials and localized separation, while the outlet region experiences intensified erosion due to high relative velocities pushing sediment particles towards the outer diameter. These localized erosion effects result in non-uniform material loss, posing serious challenges for repair and maintenance, while significantly compromising the efficiency and operational reliability of hydro turbines.

Initial studies on sand erosion damage in hydraulic machinery focused on material properties, design aspects, and hydraulic performance. Computational analyses, as reported in previous research, have enabled predictions of erosion rates for various Francis turbine components—including stay vanes, guide vanes, and runner blades—under different particle shapes, sizes, concentrations, and operating conditions. Further investigations using Computational Fluid Dynamics (CFD) with built-in erosion models such as those by Finnie, and Tabakoff and Grant, revealed that conventional hydraulic designs could be modified to mitigate erosion without significantly reducing turbine efficiency. For instance, optimizing the blade angle distribution from inlet to outlet demonstrated a notable reduction in erosion. However, to evaluate both hydraulic performance and structural resilience, structural analysis in tandem with hydraulic simulation became essential. While some studies introduced a one-way fluid-structure coupling to compare design variants, such methods fall short in capturing the feedback effects between the fluid flow and structural deformation, making them inadequate for a comprehensive integrity assessment.

The significance of two-way Fluid-Structure Interaction (FSI) modeling has been recognized in recent works involving other types of hydraulic turbines and pumps. Nevertheless, its application to Francis turbines under sediment erosion conditions remains underexplored. Moreover, numerical validation in such simulations is complicated by the high sensitivity of CFD results to mesh density and distribution, making mesh independence a critical yet challenging task. The present study aims to address these computational gaps by conducting a detailed mesh sensitivity analysis for optimal blade design and employing a two-way FSI framework to assess the structural integrity of Francis runners under sediment erosion conditions. Although a steady-state flow assumption is used in the simulations, the influence of sediment erosion is fully integrated into the structural evaluation.

2. Numerical Models

2.1 CFD Model

To simulate sediment erosion within a Francis turbine under operating conditions, a Computational Fluid Dynamics (CFD) model was developed using ANSYS CFX. A single runner passage was modeled, with sediment-laden flow analyzed through Lagrangian particle tracking. The flow field was resolved by solving the Navier-Stokes equations using a finite-volume, multi-block approach.

Turbulence Modeling

Turbulence was modeled using Reynolds-Averaged Navier-Stokes (RANS) equations. While models like **k-ε** offer robustness, they are limited in handling boundary layer separation and rotating flows. For higher accuracy in such conditions, the **Shear Stress Transport (SST) k-ω** model was adopted. This model effectively captures flow separation in regions with adverse pressure gradients, which are prevalent in Francis turbine flows.

Erosion Modeling

Quartz with a spherical shape, a density of 2.65 gm/cm3, a molar mass of 1 kg/kmol, and a diameter of 0.1 mm was the material used to define the sediment. At the intake, a concentration of one thousand particles was uniformly injected at a mass flow rate of one kilogram per second. Currently, ANSYS-CFX is compatible with two models of erosion. As a function of both impact angle and velocity, the Finnie erosion model is the first of them. The erosion on the blade with Quartz-Aluminum erosion parameters was modeled in this study using the model of Tabakoff and Grant [9]. The following relation is used to derive the erosion rate E in this model.

Due to its capacity to account for complicated variables like as impact angle, velocity, and material properties, the Tabakoff and Grant model was chosen above the simpler Finnie model among the erosion models available in ANSYS-CFX. To find the erosion rate E, one uses:

$$E = k_1 . f(\gamma) . V_p^{\ 2} . \cos^2(\gamma) [1 - R_T^{\ 2}] + f(V_{PN})$$

A dimensionless function of the impact angle in radians, denoted as f(γ), and the particle impact velocity, VP, are both included in the previous equation. For any given particle/wall material combination and impact velocity, the model constants k1, RT, and f(VPN) take on different values. Tabakoff and Grant's anticipated erosion rate is clearly not a linear function of impact velocity, impact angle, and properties of both the eroding and eroded materials, as can be seen from this equation. When compared to the Finnie erosion model, the Tabakoff and Grant model is more dependable because it relies on fewer parameters.

The multiphase model utilized in this numerical study is particle transport, with the particles carried by the fluid being tracked using a Lagrangian approach. This approach integrates a set of differential equations for the particle's position, velocity, and mass to calculate its behavior as it travels through the domain.

The **Lagrangian approach** was used to track particle trajectories by integrating equations of motion and mass for each particle within the flow field.

Boundary Conditions

The model was configured using design data from the **Jhimruk Hydropower Plant**, which operates three Francis turbines (12.6 MW total output at 1000 rpm). The plant has a **net head of 201.5 m** and a **total discharge of 7.05 m³/s**. Blade profiles and boundary conditions were derived from the '**Khoj**' runner design tool, which provided geometry and operating conditions at the **best efficiency point**.

Blade Erosion and Particle Tracking

Blade erosion was assessed both **visually**, via erosion patterns, and **quantitatively**, through erosion rate density (kg·m−2·s−1)\left(\text{kg} \cdot \text{m}^{-2} \cdot \text{s}^{-1} \right)(kg·m−2·s−1). Fig. 1 shows particle trajectories and erosion concentration. Erosion was most severe at the **pressure side outlet**, attributed to high relative velocities near the runner's outer diameter.

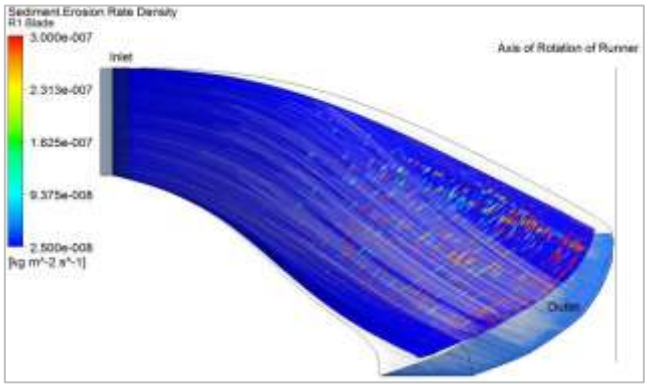

Fig 1: Erosion patterns and particle tracks

Mesh Independence Study

Mesh sensitivity was evaluated to ensure accurate prediction of erosion rates. Near-wall resolution is critical; while **y+** values between 30–100 are standard, maintaining these values requires fine meshes, especially in rotating machinery.

Using **TurboGrid, a factor ratio of 1.15** provided good near-wall resolution with acceptable mesh quality. Mesh convergence was achieved at approximately **0.75 million nodes**, as shown in Fig. 2. The final simulations used **1.25 million elements** with an RMS residual convergence of **1E-6,** ensuring accuracy.

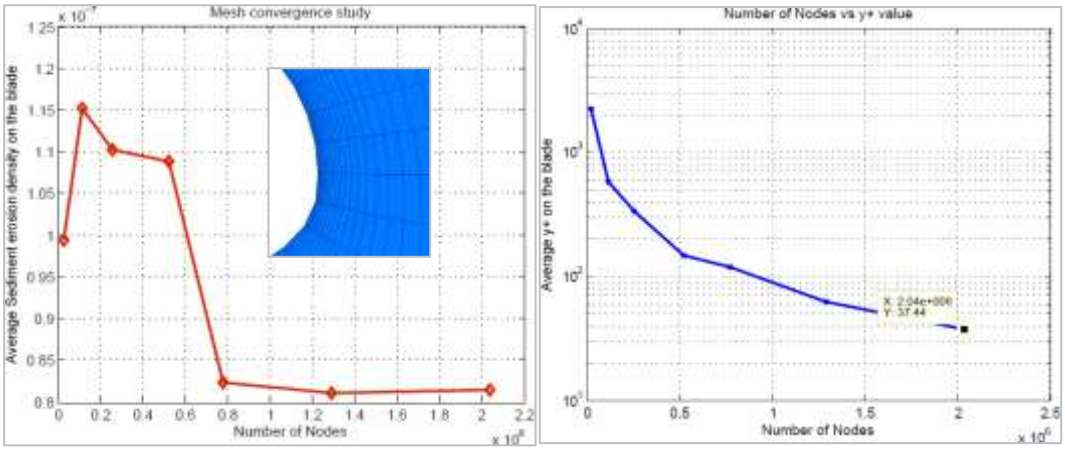

Fig 2: Mesh convergence and y+ distribution

Optimized vs Reference Blade Performance

Several optimized blade geometries, each with modified **blade angle distributions**, were analyzed and compared to a reference design (Shape 3). Changes in blade angle influence flow velocity distribution and hence erosion and efficiency.

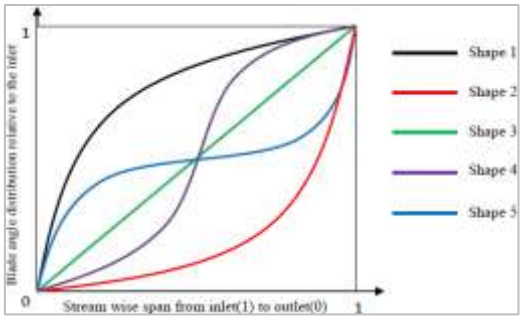

Fig 3: Blade angle configurations

All simulations used the same mesh settings. As shown in Fig. 4, while turbine **efficiency remained relatively stable** across designs, significant differences were observed in **erosion rate density**. The **Shape 4 blade** showed a **21% reduction in erosion** compared to the reference and was selected for subsequent **FSI analysis**.

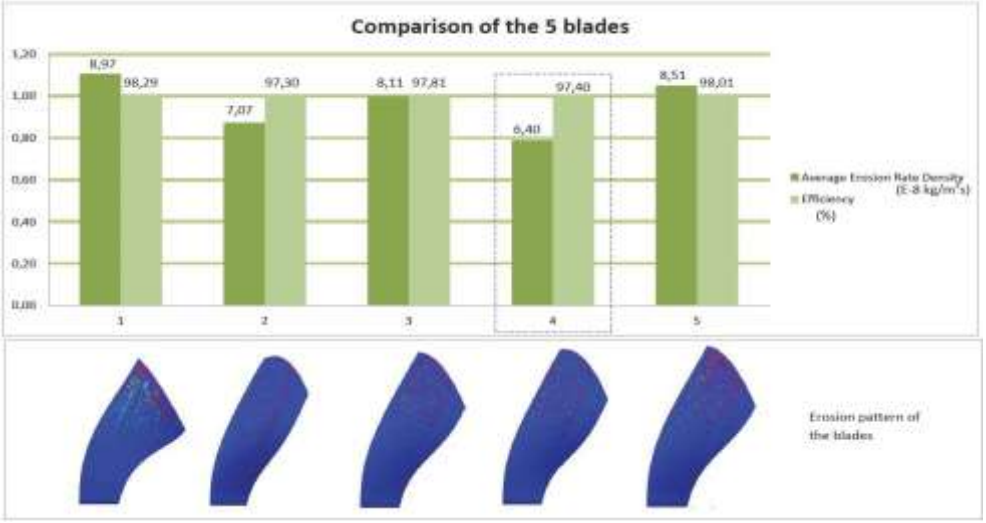

Fig 4: Comparison of erosion rates and efficiency across blade shapes

2.2 FSI Model

Fluid-Structure Interaction (FSI) refers to a coupled-field analysis in which the interactions between fluid and structural domains are simultaneously modeled to understand their interdependent behavior. In the context of **Francis turbines operating under sediment erosion conditions**, FSI becomes critical for assessing the real-time structural response of turbine components to hydraulic forces intensified by erosive particles.

There are two primary types of coupling in FSI: **one-way** and **two-way**. In *one-way coupling*, fluid forces affect the structure without feedback, while *two-way coupling* accounts for the mutual interaction between the fluid and structure, making it suitable for problems where structural deformation significantly alters fluid flow, as seen in eroded runner blades.

FSI coupling can be implemented through:

- **Direct (monolithic)** approach: solving a single system of coupled equations, offering high fidelity but at the cost of computational efficiency.
- **Iterative (partitioned)** approach: solving individual field equations and exchanging boundary data iteratively—more suitable for complex problems like those involving sediment-affected turbines.

In this study, a **two-way iterative FSI coupling** is adopted using **ANSYS MFX** (Multi-field Solver), which links **CFX (fluid domain)** and **Mechanical (structural domain)**. MFX employs **staggered iteration** where data transfer occurs cyclically between fluid and structure solvers:

- The **ANSYS Mechanical solver (master)** controls coupling, interfaces, and synchronization.
- The **CFX solver (slave)** provides the flow solution and receives structural displacement data for mesh deformation updates.

This configuration allows realistic simulation of fluid forces acting on turbine blades and corresponding deformation, especially in **sediment-laden flow environments** where erosion alters surface geometries and stress distributions.

Geometry Definition

The Francis turbine runner geometry, including the blade, hub, and shroud, was developed using CAD data in **Pro/ENGINEER**. Due to geometrical symmetry and to reduce computational costs, only one of the 17 runner sections (1 blade with corresponding hub and shroud segments) was modeled. This approach ensures proper **mapping of structural and fluid boundaries** for accurate FSI simulation.

Structural material:

- **Material**: Structural Steel
- **Density**: 7850 kg/m^3
- **Young's Modulus**: 2×10^{11} Pa
- **Poisson's Ratio**: 0.3

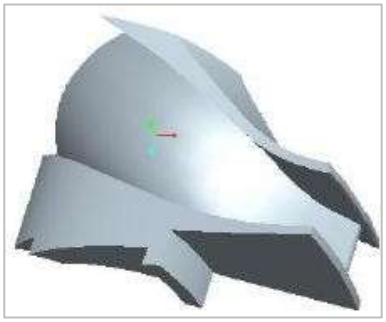

Figure 5: illustrates the final structural geometry used for FSI analysis.

Boundary Conditions

Case I – Isolated Blade Analysis

This simplified case evaluates blade behavior without considering the stiffening effects of adjacent components:

- Fixed supports at blade–hub and blade–shroud interfaces.
- Rotational velocity: 104.7 rad/s about the z-axis.
- Gravity load included.
- Fluid–structure interface defined on the blade surface.

This case provides a baseline to analyze structural integrity, stress patterns, and blade deflection under sediment-laden pressure loads. While results may underestimate stresses due to absent constraint stiffening, it is valuable for **erosion sensitivity analysis**.

Case II – Sector Model with Cyclic Symmetry

To enhance realism, this model incorporates:

- Fixed support at the shaft–hub connection.
- Fluid–structure interfaces on blade, hub, and shroud surfaces.
- Cyclic symmetry applied to represent the full runner behavior.
- Same rotational and gravitational conditions as Case I.

This approach captures the global deformation behavior and better represents **sediment-induced stress propagation across structural components**.

FSI Mesh Study

Mesh sensitivity analysis was conducted using **one-way FSI**, importing pressure loads from CFX to the structural domain. The **cyclic symmetry** was enforced using a cylindrical coordinate system ensuring mesh and geometry compatibility on sector boundaries.

- **Mapped tetrahedral mesh** for blades.
- **Unstructured mesh** for hub and shroud regions.

Mesh Convergence

- **Reference Design**: Converged at 178,575 nodes (element size: 0.0025 m).
- **Optimized Design**: Required finer mesh (~361,664 nodes; element size: 0.0028 m).
- **Full Sector Model**: Used coarser mesh (element size: 0.004 m) due to computational limits.

Mesh independence was verified via maximum equivalent stress and total deformation results (see Fig. 6). Finer meshes were especially important in capturing erosion-affected stress distributions.

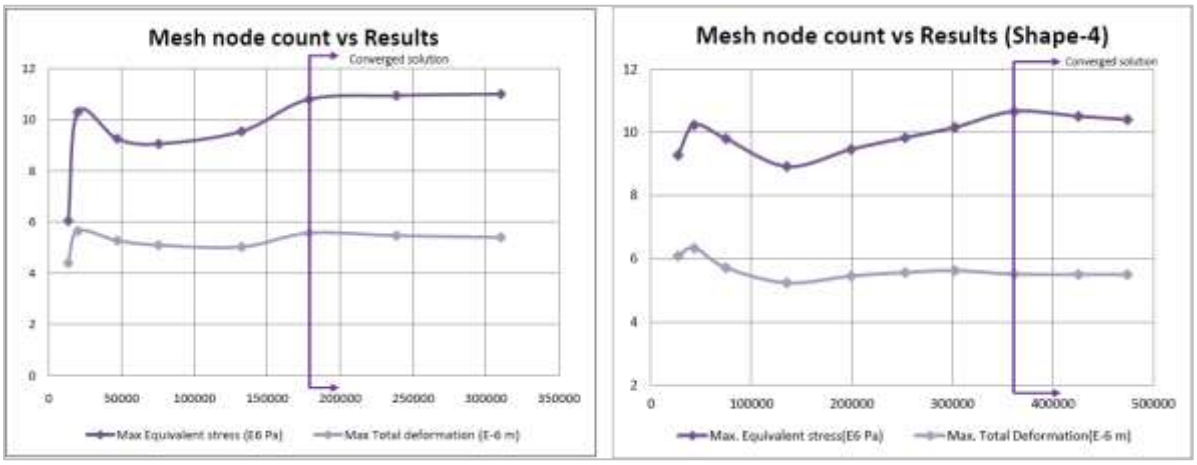

Fig 6: Mesh convergence study for structural analysis

Mesh Deformation

Mesh deformation is an important component for problems with moving boundaries or moving sub-domains. It is not considered when the steady CFD analysis was carried out. In the case of coupled FSI, this motion has to be imposed because the mesh outside the structural domain moves together with its deflection resulting in the deformation of the fluid mesh. This motion of the mesh could be determined by the mesh motion model. According to this model, the displacements applied on a boundary is diffused to mesh points with the equation,

$$\nabla.(\tau_{disp}.\nabla\delta)=0$$

Where, δ is the displacement relative to the previous mesh locations and τdisp is the mesh stiffness. This equation is solved at the start of each outer iteration. It can be inferred from this equation that the relative mesh distribution of the initial mesh has been preserved. This means that the refinement of the mesh at the boundary will remain fine after the deformation at the relative position. The value of the mesh stiffness discussed above can be controlled by choosing an appropriate value. This value can also be chosen such that the stiffness is more at the significant regions, such as near the small volumes, or near boundaries. The mesh stiffness value for this case is chosen according to the following relation,

$$\tau_{disp}=\left(\frac{1}{a*}\right)^{C_{stiff}}$$

Here a* represents either the size of the control mesh volumes, or the distance from the nearest boundary, depending upon the type of the option chosen. In any case, the stiffness of the mesh will increase when this value will decrease. The rate at which this stiffness increases depends upon the value of Cstiff which represents the model exponent. The default value of this exponent is 10, which can be altered according to the need of the problem. In the case when ANSYS Multi-field is chosen for FSI, the mesh motion can be imposed on the wall boundaries. In this case, the mesh motion has to be imposed on the blade, hub and shroud regions.

Interface Setup

Fluid–structure interaction occurs through interfaces where loads (pressure) and displacements are exchanged:

- ANSYS flags these interfaces by numeric IDs (Mechanical) or names (CFX).
- Proper **mesh alignment** at interfaces ensures accurate **bidirectional data transfer**.

CFX's **TurboGrid** generated refined meshes for fluid domains, particularly near blade edges—areas prone to sediment erosion. Ensuring compatible mesh density across both fields minimizes interpolation errors (Fig. 7).

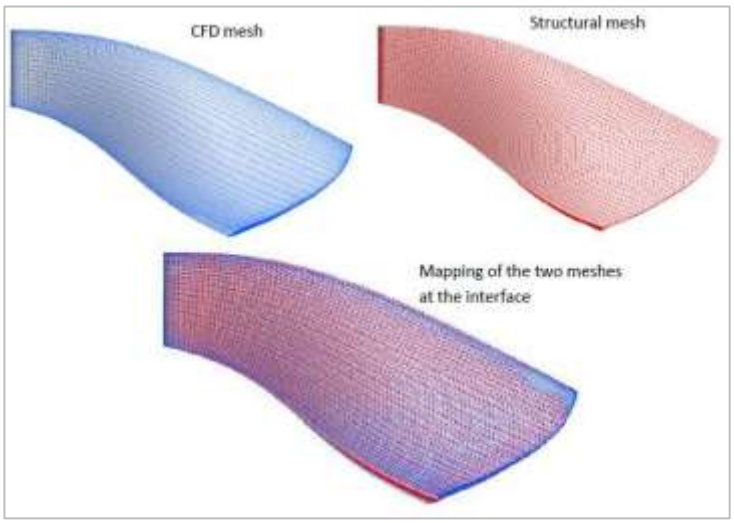

Fig7: Mesh of the two fields and mapping

Solver Setup

Staggered iterations manage field coupling in the FSI solver. At each iteration:

- Data transfer across interfaces is checked for convergence.
- Convergence is evaluated using the norm function:

$$\phi = \frac{\sqrt{\sum (u_{new} - u_{old})^2}}{\sqrt{\sum (u_{new})^2}}$$

Careful convergence control is essential to **capture the transient impact of erosion-related pressure fluctuations on blade structure**.

3. Results of Two-Way Fluid-Structure Interaction (FSI) Analysis

Case I: Blade-Only Configuration

The two-way coupled FSI analysis for the blade-only configuration under sediment erosion conditions reveals that the maximum stress occurs at the inlet region, particularly at the shroud-blade connection. The stress distribution for both reference and optimized designs is illustrated in **Figure 8**.

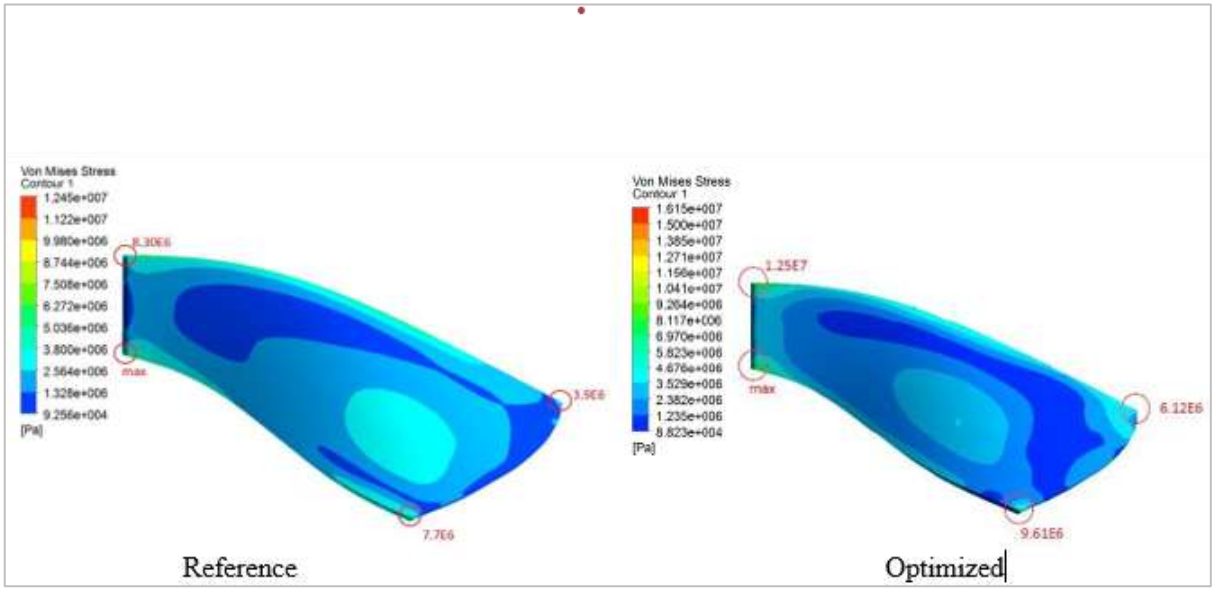

Fig 8: Stress distribution on the blade from two-way FSI

For the reference design, the peak stress is recorded at **12.45 MPa**, whereas for the optimized design, the maximum stress increases to **16.15 MPa**. Notably, high stress concentrations are observed in zero-displacement boundary regions and near the mid-span of the blade's outlet edge. These regions are critical as they are more susceptible to erosion-induced degradation under sediment-laden flow.

Case II: Full Runner Configuration

In the second case, involving the complete runner assembly (blade-hub-shroud), the two-way FSI analysis reveals a significantly different stress distribution pattern. As shown in **Figure 9**, the highest stress occurs near the blade-hub connection at the inlet region. Furthermore, elevated stress is also observed at the joint between the blade and the shroud.

The maximum stress in the reference design reaches **916.8 MPa**, while in the optimized design, it is reduced to **823.9 MPa**, indicating improved structural performance under sediment-laden flow conditions.

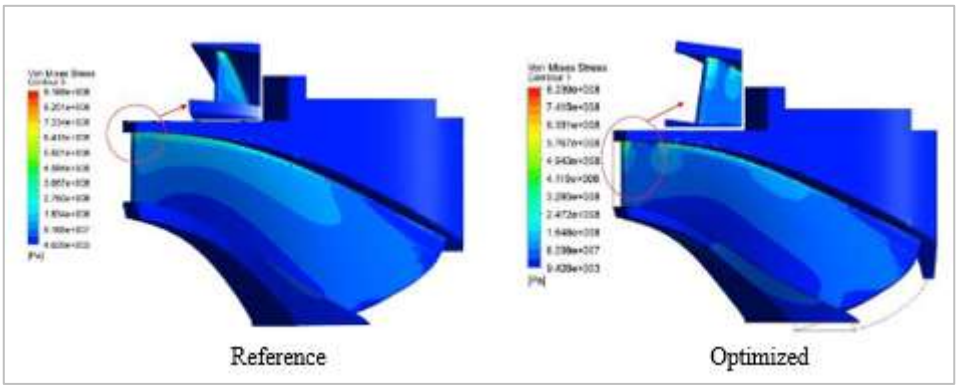

Fig 9: *Stress distribution on the runner from two-way FSI*

Mesh Deformation in Fluid Domain

The structural deformation caused by fluid interaction is reflected in the displacement of the surrounding CFD mesh. **Figure 10** presents the mesh deformation profiles around the blade at three different stream-wise locations for both designs.

In the reference design, the maximum mesh deformation occurs near the shroud region, with a peak blade deformation of **0.37 mm**. In contrast, the optimized design exhibits a different deformation pattern, with the highest displacement occurring near the inlet and mid-span of the outlet edge. Despite this shift, the maximum deformation is lower at **0.12 mm**, suggesting that the optimized configuration better withstands erosion-induced loading.

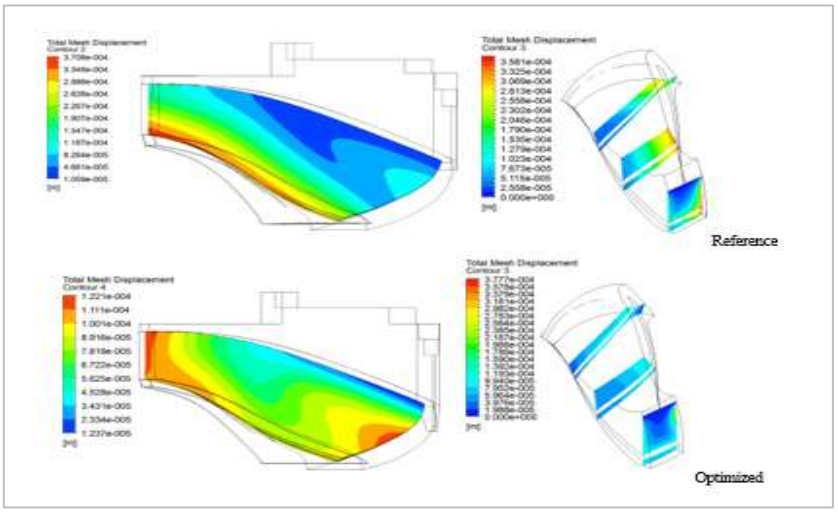

Fig 10: *Mesh deformation in the fluid domain from two-way FSI*

4. Conclusion

This study employed advanced computational techniques to optimize the design of a Francis turbine runner with respect to sediment erosion, hydraulic efficiency, and structural integrity under erosive operating conditions. Computational Fluid Dynamics (CFD) analysis was conducted on a single blade passage, utilizing boundary conditions derived from a MATLAB program developed in prior work, alongside the Tabakoff erosion model implemented within ANSYS CFX. Among the five blade geometries evaluated, Shape-4 demonstrated superior performance in minimizing sediment erosion without compromising turbine efficiency, and was therefore selected for detailed Fluid-Structure Interaction (FSI) analysis.

Two-way FSI simulations were performed on the runner section under two scenarios: the first modeled a single blade excluding the effects of blade joints and neighboring blades, while the second analyzed a sector of the full runner applying cyclic symmetry to account for interactions among blades. A mesh independence study was carried out for the single-blade case using a mapped tetrahedral mesh with one-way FSI coupling. For the full runner sector, a fixed mesh size was employed for both reference and optimized designs.

Results revealed that the second scenario exhibited higher stress distributions on the runner due to additional loadings on the hub and shroud, compared to the single blade case. The two-way FSI results indicated that the reference design experienced lower maximum stress than the optimized design in the single-blade scenario; however, this trend reversed in the full runner sector model. Structural deflections were observed through mesh deformations, showing reduced deflection in the optimized blade compared to the reference, suggesting improved structural performance.

This work presents a comprehensive methodology for addressing coupled multi-physics problems in Francis turbines using commercial software tools. The structural integrity of the turbines was evaluated through a combined assessment of erosion resistance and hydraulic efficiency via CFD, along with mechanical strength through two-way FSI analysis. The application of cyclic symmetry effectively reduced computational demands during mesh independence studies without sacrificing accuracy.

The methodologies developed herein are broadly applicable to similar multi-disciplinary engineering problems involving fluid-structure interactions under erosive conditions. Furthermore, the insights gained from this study lay the groundwork for future transient two-way coupling analyses that incorporate the dynamic effects of stationary guide vanes, enhancing the predictive accuracy of turbine performance and durability under real operating environments.

References

1. H. P. Neopane, "Sediment erosion in hydro turbines," NTNU, 2010.
2. B. Thapa, R. Shrestha, P. Dhakal, and B. S. Thapa, "Sediment in Nepalese hydropower projects," *The Great Himalayas: Climate, Health, Ecology, Management and Conservation*, 2003.
3. M. Eltvik, B. S. Thapa, O. G. Dahlhaug, and K. Gjosaeter, "Numerical analysis of effect of design parameters and sediment erosion on a Francis runner," in *Proc. Fourth International Conference on Water Resources and Renewable Energy Development in Asia*, Thailand, 2012.
4. J. B. Paulsen, "FSI-analysis of Francis turbine," NTNU, Norway, 2012.
5. H. Schmucker, F. Flemming, and S. Coulson, "Two-Way Coupled Fluid Structure Interaction Simulation of a Propeller Turbine," *International Journal of Fluid Machinery and Systems*, vol. 3, no. 4, pp. 342–351, 2010.
6. X. Huan, L. Houlin, T. Minggao, and C. Jianbao, "Fluid-Structure Interaction Study on Diffuser Pump with a Two-Way Coupling Method," *International Journal of Fluid Machinery and Systems*, vol. 6, no. 2, pp. 87–93, 2013.
7. M. Eltvik, B. S. Thapa, O. G. Dahlhaug, and K. Gjosaeter, "Numerical analysis of effect of design parameters and sediment erosion on a Francis runner," *International Journal of Hydropower and Dams*, ASIA-2012.
8. ANSYS, *ANSYS CFX-Solver Theory Guide*, Release 11.0, 2006.
9. ANSYS, *Solver Theory Guide*, Release 11.0, 2006.
10. B. S. Thapa, M. Eltvik, K. Gjosaeter, O. G. Dahlhaug, and B. Thapa, "Design optimization of Francis runners for sediment handling," in *Proc. Water Resources and Renewable Energy Development in Asia*, Thailand, 2012.
11. ANSYS, *ANSYS Coupled-Field Analysis Guide*, Release 10.0, 2005.
12. R. Negru, L. Marsavina, and S. Muntean, "Analysis of flow induced stress field in Francis turbine," *Bulletin of the Technical Institute of Iasi*, 2011.
13. R. Negru, S. Muntean, L. Marsavina, R. Susan-Resiga, and N. Pasca, "Computation of stress distribution in a Francis turbine runner induced by fluid flow," in *Proc. International Workshop on Computational Mechanics of Materials*, 2011.
14. R. A. Saeed, A. N. Galybin, V. Popov, and N. O. Abdulrahim, "Modeling of the Francis turbine runner in power stations. Part II: Stress Analysis," *WIT Transactions on The Built Environment*, vol. 105, 2009.
15. S. Lais, Q. Henggeler, U. Weiss, E. X., and E. Eguasquiza, "Dynamic analysis of Francis runners—experiment and numerical simulation," *International Journal of Fluid Machinery and Systems*, vol. 2, no. 4, pp. 303–314, 2009.